

Dental Image Segmentation by robust Clustering Methods

Carlos Balsa and Ronan Guivarc and Sandrine Mouysset

Abstract Dental image-processing, specially dental X-ray, has many applications in forensic odontology and in many fields of medicine. Segmentation of dental radiography allows the identification of human individuals but also could be used for the development of more effective diagnostic, monitoring and evaluation of appropriate treatment plans. In practice, dark background and bones tissues are not distinguished with contour extraction methods on dental images. So we propose to first apply k -means method and then to extract the contours on the clustering result. In this paper, we present an initialization of the k centroids based on the grey scale histograms, a weighted norm which includes both grey scale and geometrical informations and test it on dental X-ray images. Then we describe a promising parallel clustering method based on kernel affinity.

1 Introduction

Dental radiography is the most common way to get image of teeth. The X-ray images contain many information that can be extracted through techniques of digital image processing where the most important procedure is image segmentation. Image-processing procedure are used in computer applications such as human identification systems or assisting in clinical aspects like dental diagnosis systems and dental treatment systems [16].

Carlos Balsa

Instituto Politécnico de Bragança (IPB), Centro de Estudos de Energia Eólica e Escoamentos Atmosféricos (CEsA) da Faculdade de Engenharia da Universidade do Porto (FEUP), Portugal, e-mail: balsa@ipb.pt

Ronan Guivarc

Université de Toulouse - INPT(ENSEEIHT) - IRIT, e-mail: Ronan.Guivarc@enseeiht.fr

Sandrine Mouysset

Université de Toulouse - UPS - IRIT, e-mail: sandrine.mouysset@irit.fr

The dental X-ray is a valuable tool in forensic odontology which is a branch of forensics concerned with identifying human individuals based on their dental feature prior and after death. Unlike other biometric identifiers, the teeth are not affected by the early decomposition of body tissues after death. For this reason, teeth are specially used as biometric identifiers of human cadaver under adverse circumstances encountered in mass disasters (tsunamis, airplane crashes,...) or when identification takes place a long time after the death [18].

The use of dental biometry in forensic identification requires a *ante-mortem* and *post-mortem* radiography that are both segmented and compared for identification of undefined victims [4]. The comparison on the contour/shape of corresponding individual tooth would require reliable segmentation technique that can extract the morphology of each individual tooth from gum, bone and other body tissues [18].

The segmentation of teeth from the digital image is then a key step of identification. It is important to find an efficient and adaptable method in order to obtain an automatic segmentation process. This requirement is even more important when there is a lot of information to be processed.

Dental image-processing has other fields of application in medicine. Segmentation of dental radiography allows the development of more effective diagnostic, monitoring and evaluation of appropriate treatment plans. In oral surgery, the segmentation is used to set up digitalized dental casts used in the simulation and the planning of orthodontic interventions [8]. It enables also a non-destructive evaluation that suits the simulation of endodontics, orthodontics, and other dental treatments [6]. Dental image-segmentation is also used to aid in determining areas of lesion especially the lesions below the cortical plate that are difficult to observe by the human eye [9].

Despite the diversity and quantity of applications, computer aided dental X-rays analysis is a challenging task if we want it to be automatic, or even semi-automatic. According to Shuo Li and co-authors [9], the challenging of dental X-rays analysis results from four characteristics: (1) poor image modalities: noise, low contrast, and sampling artifacts; (2) complicated topology; (3) arbitrary teeth orientation; and (4) lack of clear lines of demarcation between regions of interest.

Usually, dental image segmentation aims to achieve the two-dimensional contour/shape of the tooth or of some internal micro-structures. The automatic execution of these tasks involves the choice of the method according to the characteristics of the image. Each image point of a digital image, also called pixel, is characterized by a vector $x \in \mathbb{R}^p$ that is one-dimensional ($p = 1$) and corresponds to the grey intensity in grey scale images. This vector is three-dimensional ($p = 3$) and corresponds to the intensity of Red, Green and Blue in RGB scale images. The images used in this work are in grey scale because they result from dental radiography.

The segmentation techniques, most commonly used, can be classified into two broad categories: (1) techniques based on the homogeneity of the region, over the individualizing of the regions that satisfy a given criterion, and (2) techniques based on the detection of edges (borders) of a region, which allow tracing the boundaries between regions with different characteristics.

The methods belonging to the first category are looking for points with similar intensity values [7]. In this category, the clustering technique aims at partitioning a data set by bringing together similar elements in subsets, called clusters [12]. The similarity depends on the distance between each couple of data points and a reduced distance indicates that they are more similar.

Among the clustering techniques, k -means method [10] is a well-known method that partitions the dataset in exactly k clusters. This is achieved in a sequence of steps. In each step the cluster's centroid (arithmetic vector mean) is computed. The minimum distance between each data point and the clusters' different centroids will decide the formation of new clusters.

The algorithm presents a rather fast convergence, but one cannot guarantee that the algorithm finds the global minimum [5] and, because during the initialization, the first centroids are chosen randomly, the results can be different for one run to another. To overcome this drawback, we propose to exploit the pick and valleys from the grey scale histogram of distribution. We apply the Otsu thresholding method [14] which lead to define the initial centroids as the distinct thresholds. The k -means algorithm based on a local procedure will converge in few steps.

We propose in this paper a process using a sequence of simple steps, with few supervision, in order to improve the dental image segmentation and contour detection but also that is more robust and no subject to random initialization. We propose a weighted norm which includes both grey scale and geometrical informations of the dental X-ray to observe if the geometrical information will improve the partitioning result.

This paper is organised as follows: in section 2 we describe the dental images selected and the results of contour extraction with no treatment. In section 3, we present the k -means algorithm, how we improve its robustness, and experimental results. Section 4 mentions a parallel approach to deal with the limitations we reach when the size of the images increases. Finally we conclude and describe future work in section 5.

2 Contour extraction on dental images

In this section, the dental X-ray images are firstly described. Then, the contour detections methods are presented, tested and thus, reveal some limits.

2.1 Data Description

We select four images shown in Fig. 1 to test the algorithms. These images come from typical dental X-rays made by two Portuguese dentists and were kindly provided by them for the realization of this work. Image **rx1** is a typical image, while the three others have some particularities. The image **rx2** has very high tonalities,

rx3 is an image with high definition and **rx4** represents a devitalized tooth with fillings in the nerve channels and inside of the crown.

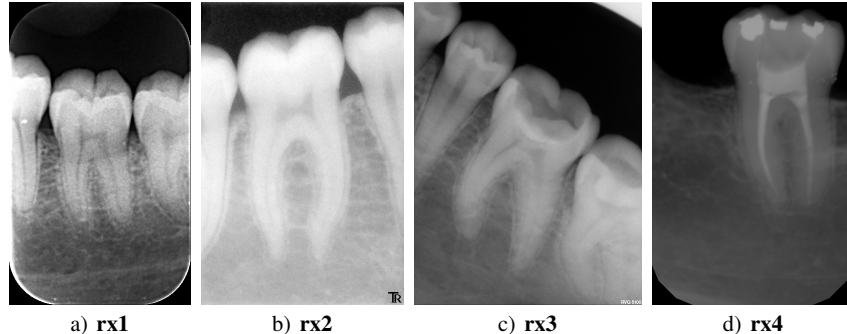


Fig. 1 Test images.

The **rx1** image has 612×366 pixels, **rx2** has 768×512 pixels, **rx3** has 1600×1200 and **rx4** has 1536×1023 pixels. All images are in grey scale with tonality values that ranges from 0 to 255, where 0 corresponds to black and 255 to white. We can present the number of pixels with the same intensity level in a histogram. The Fig. 2 contains this grey scale histogram corresponding to each test image.

In all histograms of Fig. 2 one can see a large number of pixels with very low tonality. These pixels are part of the dark background of the image.

If we shift the scale to the right we find another high frequency of tonality corresponding to the bone tissue. Its value range varies from image to image and depends from the X-ray process, especially in light intensity. For the images **rx1**, **rx3** and **rx4** the tonality of the bone tissue is between 50 and 100 and for **rx2** is between 250 and 200. The difference is due to the fact that **rx2** is much brighter than the other images.

Continuing to shift to the right, we found another peak frequency which corresponds essentially to the tooth region. This peak may be more or less close to the peak corresponding to the bone. For instance, the two peaks are close in **rx2** and **rx4** while they are more distant in **rx1** and **rx3**. We also observed that between the two tonality values, corresponding to bone and tooth, there are values with high frequencies, making hard the distinction between the two regions. In the right part of the **rx4** histogram there are several smaller peaks that indicate the existence of small regions with light colour, probably due to filling material in the tooth.

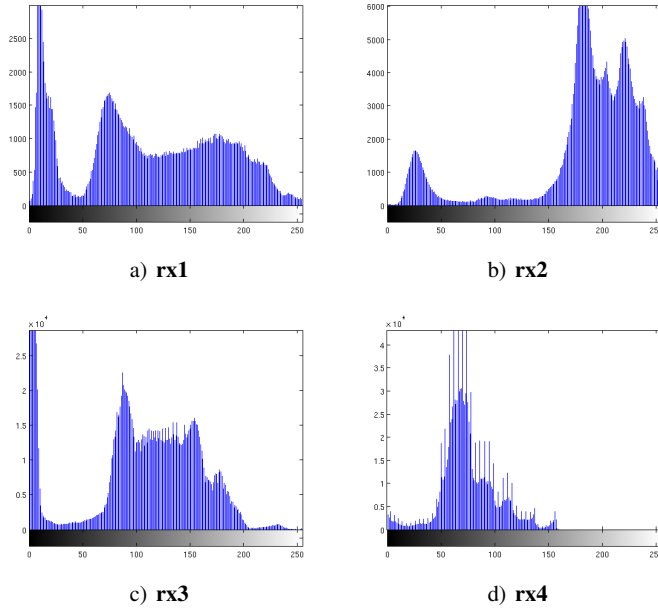


Fig. 2 Grey scale histograms.

2.2 Contour detection methods

The methods that we have used in this work to detect the contour of the teeth are also known as edge detection methods and are included in the function `edge` of the MATLAB Image Processing Toolbox (IPT). These methods detect the points corresponding to the meaningful discontinuities in the intensity values. Such discontinuities are detected by using the gradient or the Laplacian of the intensity function of the image. These approaches correspond to search points with hight values of the gradient function or zero crossing points of the Laplacian function. We present here a short survey of the main edge detectors methods.

If the function $f(x,y)$ gives the grey intensity value for each point with coordinate (x,y) , the corresponding gradient function will be defined by the following vector:

$$\nabla f = \begin{bmatrix} g_x \\ g_y \end{bmatrix} = \begin{bmatrix} \frac{\partial f}{\partial x} \\ \frac{\partial f}{\partial y} \end{bmatrix} \quad (1)$$

The magnitude of this vector is given by the corresponding norm $\|\nabla f\|$. To simplify the computations, the magnitude is sometimes computed using approximated standard norms. The magnitude of the gradient has the same behaviour as the derivatives. It is zero in regions of constant intensity and its value changes proportionally to the degree of intensity variation in regions with different grey tonalities. When

the gradient vector is non zero at coordinate (x, y) , it points always in the direction of the maximum variation of the intensity function $f(x, y)$. The maximum rate of change occurs at the angle:

$$\alpha(x, y) = \tan^{-1} \left(\frac{g_x}{g_y} \right) \quad (2)$$

The main differences between edge detection methods are how to estimate the derivatives $\partial f / \partial x$ and $\partial f / \partial y$. Since the domain is digital (discrete), derivatives in a point with coordinate (x, y) are approached by finite differences.

In the **Roberts method** [17] the derivatives are computed taking into account sets of 2×2 points

$$\begin{aligned} g_x &\approx f(x+1, y+1) - f(x, y) \\ g_y &\approx f(x+1, y) - f(x, y+1) \end{aligned} \quad (3)$$

The Roberts contour detector is the simplest and the oldest method used to detect edges. It is mainly used to detect diagonal edges. However, its efficiency is limited because it uses a small number of points to detect the variation of intensity.

In the **Prewit method** [15] the first derivatives in a point with coordinate (x, y) are computed taking into account the set of 3×3 neighbouring points.

This approach includes the nature of the data on opposite sides of the center point, with coordinate (x, y) , and thus carry more information regarding the direction of an edge [7].

The **Sobel method** [19] is similar to the Prewit method. There are only small differences in the coefficients used to approach the first derivatives. It uses a weight of 2 in the center coefficient which provides better noise-suppression and consequently image smoothing [7].

All the previous edge detector methods are based on a specified thresholding of $\|\nabla f\|$. The **Canny method** [3] has a slightly different approach. The gradient is computed using the derivatives of a Gaussian filter, instead of computing the gradient directly from the intensity function $f(x, y)$. This filter is defined by the Gaussian function

$$G(x, y) = \exp \left(-\frac{x^2 + y^2}{2\sigma^2} \right) \quad (4)$$

where σ is the standard deviation. After, the image is smoothed using the Gaussian filter, to reduce the noise, the magnitude of the gradient and the edge direction, equation (2) are computed at each point in order to find all the edges. The determined edge points are classified as strong or weak edges according to the position of the gradient magnitude comparatively to two different thresholds T_1 and T_2 , previously fixed. The Canny method returns the strong edges and weak edges that are connected with them.

Another approach to detect points with meaningful changes in the intensity values is based on the idea of finding the zeros of the second derivatives. This idea is exploited in the **LoG method** [11] that consists in computing Laplacian of filtered

image. The Laplacian of the Gaussian function (equation (4)) is

$$\nabla^2 G(x,y) = \left[\frac{x^2 + y^2 - 2\sigma^2}{\sigma^4} \right] \exp\left(-\frac{x^2 + y^2}{2\sigma^2}\right) \quad (5)$$

The expression in equation (5) is called the *Laplacian of a Gaussian* (LoG). The convolution of the intensity function of the image $f(x,y)$ with the LoG filter $\nabla^2 G(x,y)$ has two effects. The first is that the image is smoothed (the noise is reduced), the second is that the Laplacian is computed, which yields a double-edge image. The localization of the edges is achieved by finding the zeros crossings between the double edges.

Edge detectors that are based on the same concept as LoG method but where the convolution is carried out using a specific filter function different from the Gaussian are called **zero-crossing detectors** [7].

2.3 Limits of contour detection on dental images

We test these methods with the four dental images using MATLAB toolbox. The function to detect contours is the function `edge`. We choose to use `edge` with no adjustment of the threshold parameter; we remind that our goal is to have an automatic process, so we don't want to tune this parameter.

The results are similar with the four examples and can be divided in two categories:

1. results where there is too many edges (canny, log, zerocross) (see Fig. 3, on each figure the edges are printed in red over the original image `rx3`),
2. results where there is not enough edges (prewitt, roberts, sobel) (see Fig. 4),

In both situations, the results are unusable. Dark background and bones tissues are not distinguished with contour extraction on dental images. We present in the next section how a segmentation of the images before the edge detection can be useful.

3 Dental image segmentation with clustering techniques

In the following, k -means, one of the most important clustering method, is presented. Then an initialization based on the dental images and a weighted norm which includes the geometrical coordinates are proposed and then tested on images.

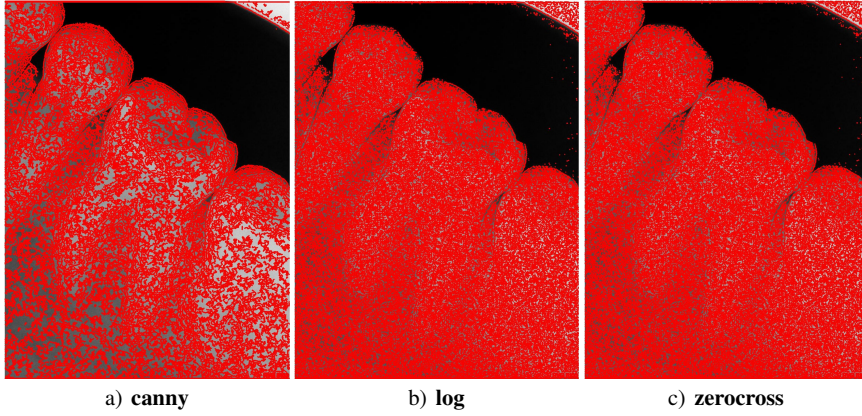


Fig. 3 Results with too many edges

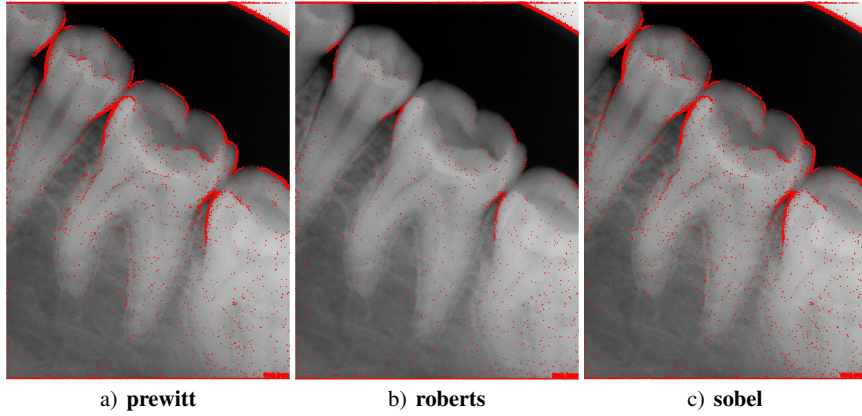


Fig. 4 Results with not enough edges

3.1 *k-means algorithm*

We are concerned with n data observations $S = \{x_i, i = 1..n\} \in \mathbb{R}^p$ that we want classify in k clusters, where k is predetermined. We organize the data as lines in a matrix $X \in \mathbb{R}^{n \times p}$. To describe the k -means method as proposed in [5], we denote a partition of vectors x_1, \dots, x_n in k clusters as $\Pi = \{\pi_1, \dots, \pi_k\}$ where

$$\pi_j = \{q : x_q \in \text{cluster } j\}$$

defines the set of vectors in cluster j . The centroid, or the arithmetic mean, of the cluster j is:

$$m_j = \frac{1}{|\pi_j|} \sum_{\ell \in \pi_j} x_\ell \quad (6)$$

where $|\pi_j|$ is the number of elements in cluster j . The sum of the squared distance, in a given norm, between the data points and the j cluster's centroid is known as the *coherence*:

$$E_j = \sum_{q \in \pi_j} \|x_q - m_j\|^2 \quad (7)$$

The closer the vectors are to the centroid, the smaller the value of E_j . The quality of a clustering process can be measured as the *overall coherence*:

$$E(m_1, \dots, m_k) = \sum_{j=1}^k E_j \quad (8)$$

The k -means is considered as an optimization method because it seeks a partition process that minimizes $E(m_1, \dots, m_k)$ and, consequently, finds an optimal coherence. The problem of minimizing the *overall coherence* is NP-hard and, therefore, very difficult to achieve. The basic algorithm for k -means clustering is an iterative two-step heuristic procedure. Firstly, each vector is assigned to its closest group. After that, new centroids are computed using the assigned vectors. In the following version of k -means algorithm, proposed by [5], these steps are iterated until the changes in the *overall coherence* are lower than a certain tolerance.

Algorithm 1 The k -means algorithm

1. Start with k initial centroid vectors $m_j^{(0)}$ for $j = 1, \dots, k$. Compute $E(m_1^{(0)}, \dots, m_k^{(0)})$. Put $t = 1$.
 2. For each vector x_i find the closest centroid. If the closest centroid is $m_p^{(t-1)}$ assign x_i to $\pi_p^{(t)}$.
 3. Compute the centroids $m_j^{(t)}$ for $j = 1, \dots, k$ of the new partitioning $\Pi^{(t)}$.
 4. If $|E(m_1^{(t)}, \dots, m_k^{(t)}) - E(m_0^{(t-1)}, \dots, m_k^{(t-1)})| < \text{tol}$, stop; Otherwise $t = t + 1$ and return to step 2.
-

Since it is a heuristic algorithm there is no guarantee that k -means will converge to the global minimum. A deterministic version of k -means, called Global k -means [2, 1], is a variant of k -means that does not depend on any initial positions for the cluster center and with the local search of k -means at each step, it provides excellent results in terms of the mean square clustering error criterion or overall coherence E . But with images with high dimension, the computational complexity and the memory cost are too important when using MATLAB.

3.2 Initialization

The k -means algorithm based in a local search procedure suffers from its sensitivity with initial conditions on the centroids. To avoid this issue, it is common to run it multiple times, with different starting conditions choosing the solution with the smaller E (m_1, \dots, m_k) but it is still not robust as we can see in Fig. 5 where we present the results of two runs of k -means on images **rx2** and **rx3** ($k = 4$) with the same input parameters.

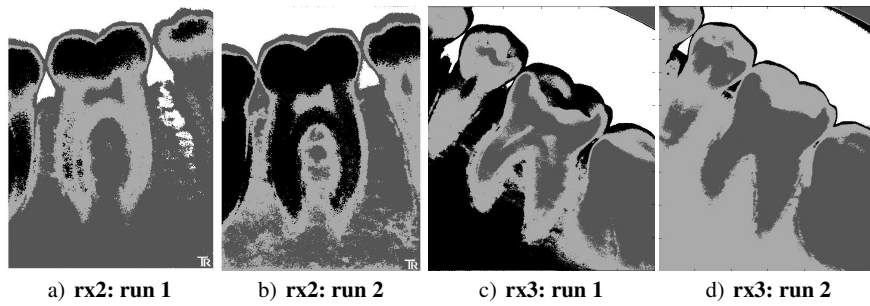


Fig. 5 Two results of k -means on **rx2** and **rx3**

We propose to exploit the histograms of dental images (cf. Fig. 2) to define the initialization of the centroids. We use a thresholding method, called Otsu's method [14], to fix initial centroids with respect to the grey scaled distribution of the image. Peaks and valleys of the image histogram are exploited for choosing the appropriate value for the thresholds T_1 and T_2 . Global thresholding, using multiple thresholds T_1, T_2 , create an image G from the data image I such that:

$$G(i, j) = \begin{cases} a & \text{if } I(i, j) > T_2 \\ b & \text{if } T_1 \leq I(i, j) \leq T_2 \\ c & \text{if } I(i, j) < T_1. \end{cases} \quad (9)$$

Otsu's multiple thresholding, as k -means, is based on the interclass variance maximization in the sense that well thresholded classes have well discriminated intensity values. Each centroid will represent a threshold from the Otsu method.

As the k -means algorithm is based in a local search procedure, Otsu's method conditions the segmentation in an optimized way. The minimization of the overall coherence E with this initialization permits extracting more information in the clusters specially when the dental X-ray presents some difficulty as shown in Fig 1 with the depth of **rx3** and the restoration materials of **rx4**.

3.3 About the norms

When dealing with grey-scale images, one have the possibility to use different norms to measure the distance among the elements of a data set in segmentation algorithms.

Let us consider an image I of size $l \times m$ and denote a pixel p as a triplet (i, j, I_{ij}) where (i, j) are the coordinates of the pixel in I and I_{ij} its grey intensity.

Norms where only the grey intensity I_{ij} is taking into account can be considered. For instance MATLAB k -means function permits us to choose between the L_1 -norm (called City-Block norm) or the L_2 -norm (or Euclidian norm). The distance between two pixels $p = (i, j, I_{ij})$ and $p' = (i', j', I_{i'j'})$ is then computed by

$$d_1(p, p') = |I_{ij} - I_{i'j'}| \quad (10)$$

for the L_1 -norm and

$$d_2(p, p') = \|I_{ij} - I_{i'j'}\|_2 \quad (11)$$

for the L_2 -norm. In practice, the clustering results with either the L_1 or L_2 norm are exactly the same. So in the following, we will show the resulting segmentation with norm d_1 .

But one may consider norms where the geometry of the image is also taking into account. Then, the resulting clusters of the segmentation algorithms will group pixels with close grey intensity but also that are close to each others in the image. Norms that include both grey intensity and geometry can be defined with a weight on each part. In the experiments, we use the following norm to compute the distance between two pixels p and p' :

$$d_G(p, p') = \alpha \left(\left(\frac{i-i'}{l} \right)^2 + \left(\frac{j-j'}{m} \right)^2 \right)^{\frac{1}{2}} + \beta \left| \frac{I_{ij} - I_{i'j'}}{256} \right| \quad (12)$$

3.4 Experimental results

The analysis of histograms (Fig. 2) allowed us to identify three main grey tonality, corresponding to the three main regions of the images: tooth, bone and dark background. Based on this observation we apply the k -means method to separate the image pixels into three clusters for **rx1** and is plotted Fig. 6.

As expected, the three clusters correspond mainly to the principal image areas, namely the tooth, bone tissue and the dark background. Cluster 1 includes most of the teeth as well as the small pieces of bone tissue that are lighter. Cluster 2 includes most of the bone tissue as well as the most shaded parts of the tooth, particularly the crown and the pulp cavity. Cluster 3 includes only the background image around the crown. This last area can be used to define the contour of the tooth crown.

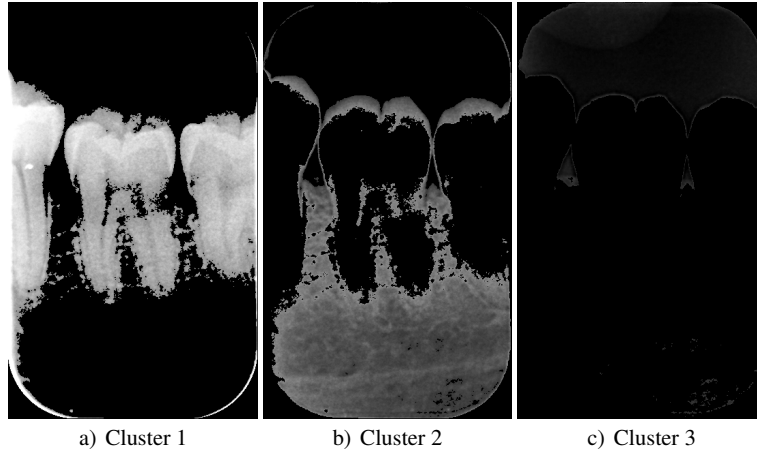


Fig. 6 Segmentation of **rx1** by k -means in 3 clusters.

In the following, we apply the Sobel method (unless mentioned) for the contour detection on the clustering results from k -means for all the test images (we observe that after segmentation, the results are roughly the same regardless of the edge detection method used). We plot on the original image the detected contours in red color in Fig. 7 for results with the norm d_1 and norm d_G . The parameters α and β of the norm d_G are 0.05 and 0.95 (the results are very sensitive to these values and the geometric part has to be small).

The results obtained by classifying into 3 clusters **rx1** show that the contours which separate the clusters 2 and 3 fail to perfectly separate the bone from the tooth. This is due to the similarity between tonalities in both parts of the image. All pixels with similar tonality values are included in the same cluster, regardless of their position in the image.

The contours resulting from the clustering of **rx2** in three clusters are shown in Fig. 8. It is noted that although **rx2** having tonalities of tooth and bone regions very close (see Fig. 2 b)), the division into three regions permits separate much of the tooth from the bone tissue. The contour of the first and the second clusters contain a large part of respectively the tooth and the bone. As had already been observed for **rx1**, the segmentation of the tooth fails especially around the roots where small lighter areas of bone are affected to the bone region. It fails also in the top of the crown and in the pulp cavity due to darker tonalities of the pixels in these area. The use of norm d_G suppresses some noise around the contours of the tooth.

Image **rx3** presents a different angle of incidence of the rays. Fig. 9 shows the four regions resulting from the segmentation of the image **rx3** by k -means method.

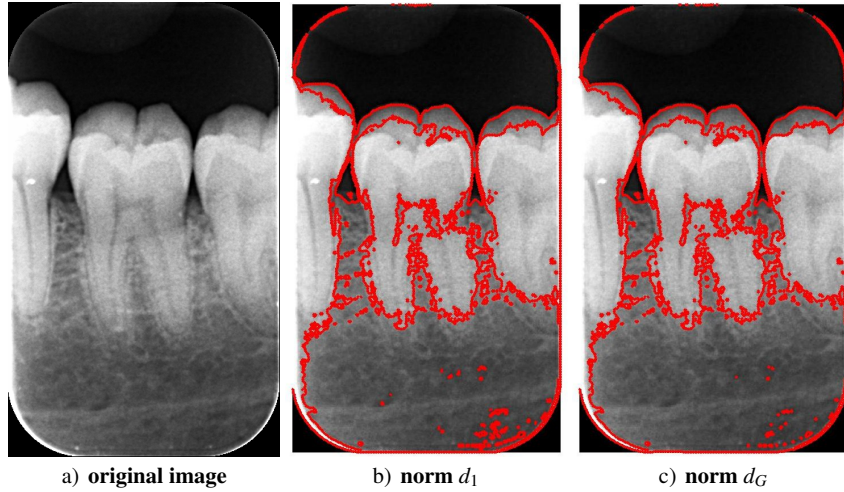


Fig. 7 Results with image rx1 ($k = 3$)

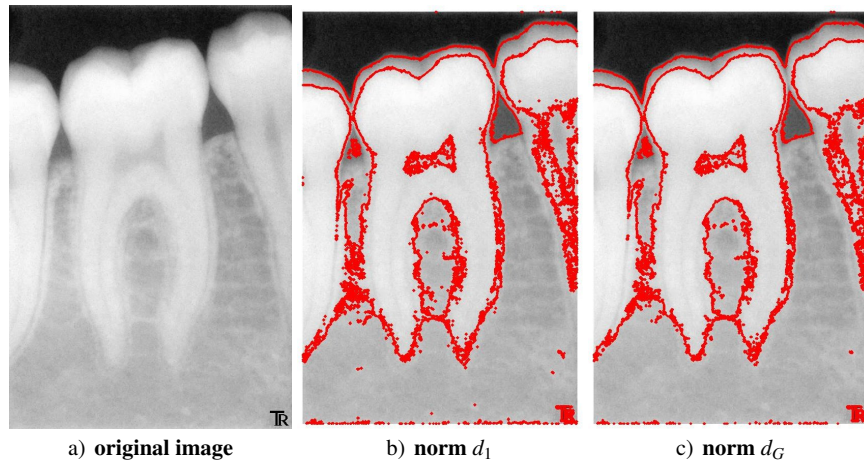


Fig. 8 Results with image rx2 ($k = 3$)

Compared with previous images, the separation between the tooth and bone tissue in the root zone is well achieved. This may be due to the high resolution of the image resulting in a smoother variation in the tonalities of grey, which better differentiate the various structures resulting from the X-ray. The use of geometrical distance filters some noise around the root canals.

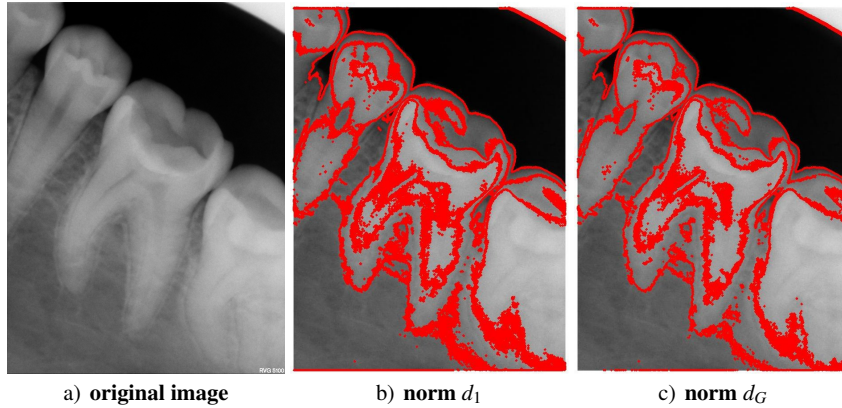


Fig. 9 Results with image rx3 ($k = 4$)

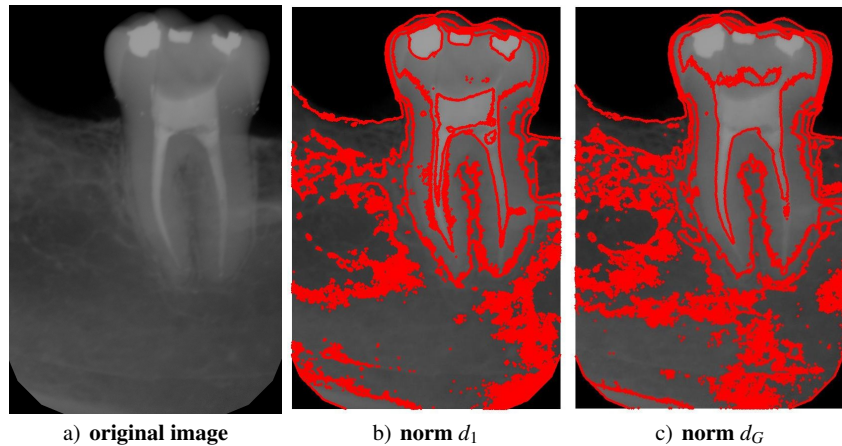


Fig. 10 Results with image rx4 ($k = 6$)

The tooth shown in the image rx4 is devitalized. As it includes material restoration, the image is segmented in six clusters and the detected contours are plotted in Fig.11. This result shows that k -means is appropriate to isolate the morphology of dental restorations for the norm d_1 (or d_2) (Fig. 10 b) whereas the filling of root canals and crown restoration materials are included in the cluster associated with the tooth when the segmentation is made in tree clusters (Fig. 10 c)).

Results on image rx4 with the norm d_G for $k = 6$ show that the crown restoration material is not captured although it is done with norm d_1 . So we try higher values of k to evaluate when those parts are detected. We obtain the value $k = 12$ (see Fig. 11) with Sobel method. If we use now the Canny method, $k = 10$ is sufficient to detect

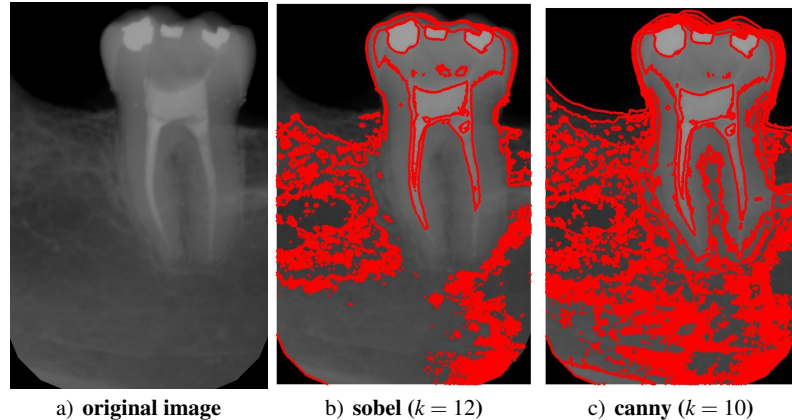


Fig. 11 results with image rx4 with sobel and canny filter

those restorations but we observe some noise at the bottom of the image. In Fact, we find the behaviour of the edge detection methods mentioned in section 2.3 but with some good results in the interesting parts of the image.

4 On clustering methods with kernel affinity: parallel spectral clustering

The k -means algorithm with Euclidean measure could only create linearly separated clusters. But kernel affinity, for example Gaussian affinity defined by equation (4), are useful when considering non-convex shaped subsets of points.

In that sense, spectral clustering aims at selecting dominant eigenvectors of a parametrized Gaussian affinity matrix in order to build an embedding space in which the clustering is made. The drawback of clustering method is that the complete affinity matrix should be computed. And the memory cost and the computational complexity lead to adapt this method for parallelization with a divide and conquer strategy [13] in a FORTRAN code with MPI parallel environment.

By exploiting the topology of images, clustering can be made on subdomains by breaking up the data set into data subsets with respect to their geometrical coordinates in a straightforward way. With an appropriate Gaussian affinity parameter [12] and a method to determine the number of clusters, each processor applies independently the spectral clustering on a subset of data points and provides a local partition on this data subsets. Based on these local partitions, a grouping step ensures the connection between subsets of data and determines a global partition.

At the grouping level, spectral clustering algorithm is made on a subset with geometrical coordinates close to the boundaries of the previous subdomains. This

partitioning will connect together clusters which belong to different subdomains thanks to the transitive relation.

As the image is divided in data subset according to the geometrical coordinates, we use the geometrical norm defined by equation (12). Fig. 12 presents a first result of parallel spectral clustering followed by edge detection on dental image **rx1**. The results are promising and permits us to continue this work with images of high dimension/precision.

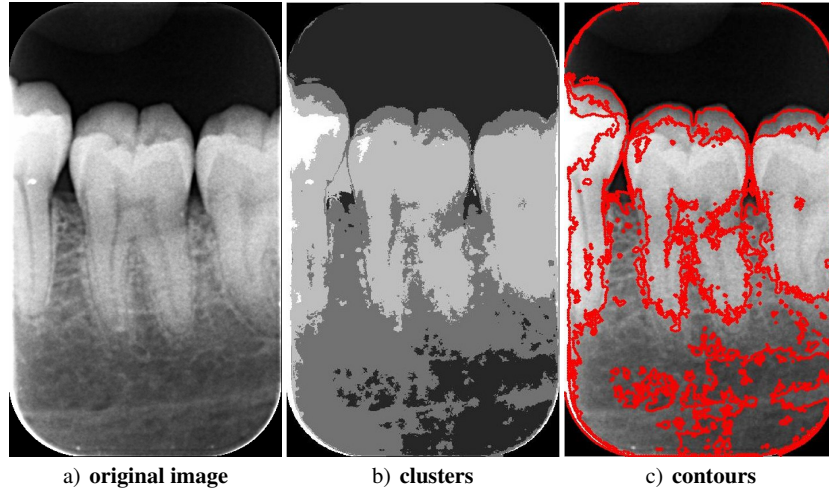


Fig. 12 results with parallel spectral clustering

5 Conclusion

The success of the segmentation depends largely on the target image. If the goal is to obtain the contour of the tooth, the existence of shaded areas, especially in the periphery, make this task difficult. The radiography performed upstream is of utmost importance. It should be taken also care in positioning and calibrating the equipment in a manner to provide the best angle of incidence of the rays. This process is responsible for the homogeneity of the regions in each of the different structures.

The k -means method allows to split the image into several parts depending on the tonality of grey. This method adapts well to the problem of segmentation of dental images where there are three dominant tonalities. The clustering into three clusters allows to divide the image into three regions: the tooth, the bone and the dark background. With the use of a larger number of clusters it is possible to isolate other structures inside the tooth, for example, the materials used in dental treatments. With

an optimal initialization of the centroids and the possibility of using a geometrical norm k -means offers different segmentations which lead to detect more precisions in the contours with classical methods such as Sobel or Canny methods.

We present in this paper a sequence of simple steps to improve the robustness of k -means method with very few input parameters, essentially the number of clusters which value could be fixed by an analysis of grey scale histograms.

We mention the spectral clustering method, that is a promising method when considering images with high dimension and/or precision. To be able to process theses images, parallel methods, parallel spectral clustering but also a parallel Global k -means, are necessary and it is in this direction that our future work will lead.

References

1. Agrawal, A. and Gupta, H. (2013). Article: Global K-Means (GKM) Clustering Algorithm: A Survey, *International Journal of Computer Applications*, 79:2,20–24.
2. Aristidis, Likas and Nikos, Vlassis and Jakob, J. Verbeek (2003). The global k-means clustering algorithm, *Pattern Recognition*, 36:2:451–461.
3. Canny, J. (1986). A Computational Approach for Edge Detection. *IEEE Trans. Patern Anal. Machine Intell.* 8(6): 679-698.
4. Dighe, S. and Shriram, R. (2012). Preprocessing, Segmentation and Matching of Dental Radiographs used in Dental Biometrics International Journal of Science and Applied Information Technology 1(2).
5. Eldén, L. (2007). Matrix Methods in Data Mining and Pattern Recognition. *SIAM*.
6. Gao, H. and Hossain, M. J. and Chae, O. and Chen, J. X. (2008). Visualization of Tooth for non Destructive Evaluation Advanced Nondestructive Evaluation II 536-54.
7. Gonzalez, C. R. and Woods, R. E. (2008). Digital Image Processing. *Pearson Education*.
8. Kronfeld, T. and Brunner, D. and Brunnett, G. (2009). Snake-Based Segmentation of Teeth from Virtual Dental Casts Computer-Aided Design and Applications 7(2) 221-233.
9. Li, S. and Fevens, T. and Krzyżak, A. and Jin, C. and Li, S. (2007). Semi-automatic computer aided lesion detection in dental X-rays using variational level set *Pattern Recognition* 40(10):2861-2873.
10. MacQueen, J. B. (1967). Some Methods for Classification and Analysis of Multivariate Observations. Proceedings of 5-th Berkeley Symposium on Mathematical Statistics and Probability, University of California Press, 1:281-297.
11. Marr, D. and Hildreth, E. (1980). Theory of Edge of Edge Detection. *Proc. R. Soc. Lond.* B207:187-217.
12. Mouysset, S. and Noailles, J. and Ruiz, D. (2008). Using a Global Parameter for Gaussian Affinity Matrices in Spectral Clustering. *High Performance Computing for Computational Science - VECPAR 2008*, 378 - 390.
13. Mouysset, S. and Noailles, J., Ruiz, D. and Guivarch, R. (2010). On a strategy for Spectral Clustering with parallel computation, High Performance Computing for Computational Science: 9th International Conference, 2010.
14. Otsu, Nobuyuki (1975), A threshold selection method from gray-level histograms, *Automatica*, 11, 285–296.
15. Prewitt, J. M. S. (1970). Object Enhancement and Extraction Picture Processing and Psychopictorics, Lipkin, B. S. and Rosenfeld (eds), Academic Press, New York.
16. Rad, A. E. and Rahim, M. M. and Rehman, A. and Altameem, A. and Saba, T. (2013). Evaluation of Current Dental Radiographs Segmentation Approaches in Computer-aided Applications IETE Technical Review 30:210-22.

17. Roberts, L. G. (1965). Machine Perception of Three-Dimensional Solids Optical and Electro-Optical Information Processing, Tippet, J. T. (ed.), MIT press, Cambridge.
18. Said, S. and Fahmy, G. and Nassar, D. and Ammar, H. (2004). Dental X-ray Image Segmentation Proceedings SPIE 5404, Biometric Technology for Human Identification.
19. Sobel, I. E. (1970). Camera Models and Machine Perception. Ph.D. dissertation, Stanford University, Palo Alto.